GFZ

Helmholtz-Zentrum
POTSDAM

HELMHOLTZ-ZENTRUM POTSDAM
DEUTSCHES
GEOFORSCHUNGSZENTRUM

Qianxin Wang, Tianhe Xu, Guochang Xu

HALO_GPS Software User Manual

(High Altitude and LOng Range Airborne GPS Positioning Software)

Version of 2010

Scientific Technical Report STR10/11

www.gfz-potsdam.de

HELMHOLTZ
GEMEINSCHAFT

Impressum

Helmholtz-Zentrum Potsdam
Deutsches GeoForschungsZentrum

Telegrafenberg
D-14473 Potsdam

Gedruckt in Potsdam
November 2010

ISSN 1610-0956

Die vorliegende Arbeit
in der Schriftenreihe
Scientific Technical Report (STR) des GFZ
ist in elektronischer Form erhältlich unter
www.gfz-potsdam.de - Neuestes - Neue
Publikationen des GFZ

Qianxin Wang, Tianhe Xu, Guochang Xu

HALO_GPS Software User Manual

(High Altitude and LOng Range Airborne
GPS Positioning Software)

Version of 2010

Scientific Technical Report STR10/11

HALO_GPS

(High Altitude and LOng Range Airborne GPS Positioning Software)

Software User Manual

Version of 2010

Qianxin Wang, Tianhe Xu, Guochang Xu

GFZ German Research Centre for Geosciences
Department 1: Geodesy and Remote Sensing
Telegrafenberg, 14473 Potsdam, Germany

June 2010

Scientific Technical Report STR 10/11
10.2312/GFZ.b103-10119

HALO_GPS Software User Manual

Contents

1. Introduction

HALO_GPS is a precise GPS kinematic positioning software. It was developed at GFZ Potsdam for the German HALO project. The goal is to develop a software which is able to achieve cm-level accuracy for an aircraft trajectory for application in airborne gravimetry.

To fulfill the needs of the HALO project, some new algorithms and strategies are developed and adopted in this software. It can automatically choose and change reference satellite, as well as the reference station, automatically detect cycle slips, outliers, bad observation data, and potential large jumps in the receiver clock. The one-click functionality is implemented for ease of use. All process steps will be finished automatically after the user enters one command.

The development of the HALO_GPS software was started in 2009, first year for theoretical study and then for code design. It has been tested with various kinds of real data. Many comparisons have been made with several well known GPS software packages, such as Ashtech Solution, Trimble Geomatics Office, and GAMIT. The results show a strong stability and reliability of HALO_GPS. The software has been used to successfully process the GPS data of NorthGrace2007 and AlpinAero2008 airborne gravimetry campaigns.

This manual outlines the characteristics of the software and describes how to use it. The principles and new features are outlined systematically and referred partly to existing references. The major functions of some important subroutines are introduced briefly. Numerical examples of kinematic positioning and internal tests as well as external comparisons are given.

This software is developed in Fortran 90 under Unix operating system and can be used on PCs under Linux without any change. The user interface to HALO_GPS is command driven with default values for most processing. This interface provides flexibility and should make the software usable with little training.

2. Structure of Software

HALO_GPS software consists of a main function and about 50 important subroutines. Each subroutine attends to its own duties, which are connected with the main function main.f90 via the input and output parameters. Therefore, it is very important for using this software to known the definitions of input parameters, output parameters and the function of each subroutine.

2.1 Main Function

The main function is the most important part in the most of software, which is used to organize the rest of the subroutines. The main function of HALO_GPS includes 15 important steps, which are outlined below.

1. Reading Control File
2. Reading Precise Ephemeris
3. Reading Observation File of Reference Station
4. Reading Observation File of Kinematic Station
5. Scanning and Modifying All Observation Data
6. Single Point Positioning
7. Computing Receiver Clock Errors
8. Searching Common Satellites
9. Cycle Slip Detection
10. Choosing Reference Satellite
11. Forming Double Observation Equations
12. Initializing Matrixes and Ambiguities
13. Parameters Estimation with Sequential Adjustment
14. Scanning the Residuals
15. Generating Result Files and Summary

2.2 Important Subroutines

read_control_file.f90

Input parameters:
The address of control file
Example: "./Example/control_file/model_control_file_1.txt"
Output parameters:
A logical variable which represents whether the address of control file is right or not
Introduction:
This subroutine is used to read the control file defined by the user in a flexible form.
Some important variables are assigned initial values based on the definitions in the control file.
The definitions of control file will be described in Chapter 3.

read_sp3.f90

Input parameters:

The address of precise ephemeris

Output parameters:

The number of healthy satellites and their ID;

The number of lost satellites and their ID;

The number of bad satellites and their ID;

The bad satellite means the satellite clock error valued is 999999.999999;

All information is saved in the structure variable named as igs.

igs(epoch)%Rtime	------seconds at this epoch
igs(epoch)%RMJD	------Modified Julian Day at this epoch
igs(epoch)%Rx(satellite_id)	------X coordinate of this satellite at this epoch
igs(epoch)%Ry(satellite_id)	------Y coordinate of this satellite at this epoch
igs(epoch)%Rz(satellite_id)	------Z coordinate of this satellite at this epoch
igs(epoch)%Rclock(satellite_id)	------clock errors of this satellite at this epoch
igs(epoch)%Rlogical(satellite_id)	------health of this satellite

ymdhms_to_MJD.f90

Input parameters:

Year, Month, Day, Hour, Minute, Second

Output parameters:

Modified Julian Date (MJD)

Introduction:

The routine converts a calendar date with hour, minute and second to a Modified Julian date.

The calendar date is ordered as year, month, day, hour, minute and second.

These values are stored in a single I*2 array.

This routine is only valid for date after 1600 Jan 0.

The relationship between JD and MJD is: JD = MJD + 2400000.5d0

matinv.f90

Input parameters:

The original matrix

The rows of this matrix and the columns of this matrix

Output parameters:

Inverse matrix

svs_cm_to_phs.f90

Input parameters:

MJD; Satellite ID; Satellite position of the center of mass

Output parameters:

The phase center position of satellite

sun20.f90

Input parameters:

XMJD (Epoch in modified Julian date in R*8 Barycentric Dynamical Time corresponding to ephemeris time)

Output parameters:

X (K), K=1, 2, and 3: Rectangular coordinates of the sun in equatorial system J2000.0 (in AU)

R : Distance of earth-sun (in AU)

L, B : Ecliptical longitude, latitude in mean system of epoch XMJD

Introduction:

It is used to compute the position of the sun at XMJD time.

This subroutine was written using Simon Newcomb's "tables of the sun".

read_ref_obsfile.f90

Input parameters:

Address of observation file; reference station ID; start time; the number of epoch

Output parameters:

The height of antenna atthis station	---ref_i_Hant/ ref_i_Eant/ ref_i_Nant
The number of observation types	---ref_i_obstype_num
The specified types of observation	---ref_i_obstype(10)
The sampling interval	---ref_i_interval
GPS seconds at every epoch	---ref_i_G_time(epoch,1)
MJD at every epoch	---ref_i_G_time_MJD(epoch,1)
The number of satellites at every epoch	---ref_i_G_sat_num(epoch,1)
All satellites ID at every epoch	---ref_i_satnum(epoch,32)
The number of read epoch	---ref_i_read_epoch
L1	---ref_i_vobs1(epoch,sat_id)
L2	---ref_i_vobs2(epoch,sat_id)
C1	---ref_i_vobs3(epoch,sat_id)
P1	---ref_i_vobs4(epoch,sat_id)
P2	---ref_i_vobs5(epoch,sat_id)
C2	---ref_i_vobs21(epoch,sat_id)
D1	---ref_i_vobs22(epoch,sat_id)
D2	---ref_i_vobs23(epoch,sat_id)
S1	---ref_i_vobs24(epoch,sat_id)
S2	---ref_i_vobs25(epoch,sat_id)
LI	---ref_i_vobs6(epoch,sat_id)
MW	---ref_i_vobs7(epoch,sat_id)
LC	---ref_i_vobs8(epoch,sat_id)

Additional function:

Remove the abnormal observations;

Remove the observations of those satellites which belong to question satellites;

Remove the observations of GLONASS satellites;

read_kin_obsfile.f90

Input parameters:

Address of observation file; kinematic station ID; start time; the number of epochs

Output parameters:

It is similar to read the observation file of reference station.

earth_tide.f90

Input parameters:

Julian Day; XYZ coordinates of station

Output parameters:

Tidal correction to site position (m)

Introduction:

The subroutine is used to compute the solid earth tide, based on the formulations in DSR thesis with extension to the number of coefficients.

receiver_antenna_correction.f90

Input parameters:

Longitude of station; Latitude of station; Height of antenna at this station (ref_i_Hant/ ref_i_Eant/ ref_i_Nant)

Output parameters:

The corrections of receiver antenna phase centre

---ref_i_ant_x/ ref_i_ant_y/ ref_i_ant_z

---kin_i_ant_x/ kin_i_ant_y/ kin_i_ant_z

unify_obs_time.f90

Input parameters:

Reference station ID; kinematic station ID

Output parameters:

The real number of processing epochs of reference station and kinematic station

Introduction:

Firstly, this subroutine tries to find out the lost epochs in reference station and kinematic station. Then it removes these epochs from the observations of reference station which are lost in that of kinematic station and removes these epochs from the observations of kinematic station which are lost in that of reference station.

Finally, the epochs between reference and kinematic stations are arranged in a certain order.

mjd_to_ymdhms.f90

Input parameters:

Modified Julian Date (MJD)

Output parameters:

Year, Month, Day, Hour, Minute, Second

Note:

If a full Julian date is used, the resolution of the seconds will only be about 10 microseconds, and a MJD should yield a resolution of about 0.1 microseconds in the seconds.

spp_1.f90

Input parameters:

Kinematic station ID; position and clock error of satellite (the structure variable IGS)

Output parameters:

XYZ and BLH coordinates of kinematic station

---kin_i_X(epoch, 1)/ kin_i_Y(epoch, 1)/ kin_i_Z(epoch, 1)

---kin_i_B(epoch, 1)/ kin_i_L(epoch, 1)/ kin_i_H(epoch, 1)

The clock error of kinematic station

---kin_i_C(epoch,1)

Satellite elevation angle at each epoch

---kin_i_elev(epoch, sat_id)

The weight of observations

---kin_i_sat_p(epoch, sat_id)

Introduction:

This subroutine computes the initial positions of kinematic station and receiver clock errors using Pseudorange C1 based on the single point positioning.

solu_sat_xyzc.f90

Input parameters:

The transmit time of signal; Satellite ID

Output parameters:

The position and clock error of satellite

Introduction:

The subroutine uses 8 orders Chebyshev polynomial to interpolate satellite coordinates.

solu_ro_xyz.f90

Input parameters:

Epoch number; satellite ID; station mark (1=reference station; 2=kinematic station)

Output parameters:

The distance between satellite and reference station or kinematic station:

ref_i_Rox(j, sat) ref_i_Roy(j, sat) ref_i_Roz(j, sat) ref_i_R0(j, sat)

kin_i_Rox(j, sat) kin_i_Roy(j, sat) kin_i_Roz(j, sat) kin_i_R0(j, sat)

Introduction:

This subroutine computes the distances between satellite and the station taking into account the influence of earth rotation.

xyz_blh.f90

Input parameters:

XYZ Cartesian coordinates in WGS-84 system

Output parameters:

BLH Geodetic coordinates in WGS-84 system

spp_2.f90

Input parameters:

Kinematic station ID; the structure variable IGS

Output parameters:

The tropospheric delay of kinematic station at every epoch ---kin_i_trop(epoch, sat_id)

Introduction:

```
kin_i_trop(j, sat_id) = kin_i_dry_ztd(j, 1) * kin_i_dry_mf(j, sat_id)
                      + kin_i_wet_ztd(j, 1) * kin_i_wet_mf(j, sat_id)
```

met_seasonal.f90

Input parameters:

JD; Latitude; Height

Output parameters:

Temperature in Celsius; Pressure in mbar; Relative humidity; Bias in surface temperature

Introduction:

This subroutine computes the temperature, pressure and relative humidity based on the seasonal argument.

dry_saas_zen.f90

Input parameters:

Temperature; Latitude; Height; Pressure

Output parameters:

Dry zenith delay of the station

Introduction:

Routine to compute dry zenith delay based on Saastamoinen model.

wet_saas_zen.f90

Input parameters:

Temperature; Latitude; Height; Relative humidity

Output parameters:

Wet zenith delay of the station

Introduction:

Routine to compute wet zenith delay based on Saastamoinen model.

wet_press.f90

Input parameters:

Temperature; Relative humidity

Output parameters:

The partial pressure of water vapor

dry_mtt_map.f90

Input parameters:

Temperature; Latitude; Height; Elevation angle (in deg) of satellite

Output parameters:

Dry mapping function

Introduction:
Niell global mapping function is adopted.

wet_mtt_map.f90

Input parameters:
Temperature; Latitude; Height; Elevation angle (in deg) of satellite
Output parameters:
Wet mapping function
Introduction:
Niell global mapping function is adopted.

spp_3.f90

Input parameters:
Kinematic station ID; the structure variable IGS
Output parameters:
XYZ and BLH coordinates of kinematic station
---kin_i_X(epoch, 1)/ kin_i_Y(epoch, 1)/ kin_i_Z(epoch, 1)
---kin_i_B(epoch, 1)/ kin_i_L(epoch, 1)/ kin_i_H(epoch, 1)
The clock error of kinematic station
---kin_i_C(epoch,1)
Satellite elevation angle at each epoch
---kin_i_elev(epoch, sat_id)
The weight of observations
---kin_i_sat_p(epoch, sat_id)
Introduction:
This subroutine computes the initial positions of kinematic station and receiver clock error using Pseudorange C1 and the weight matrix of spp_1 solution again.
Additionally, it deletes those satellites with the low elevation angle.

ref_clock_1.f90

Input parameters:
Reference station ID; the structure variable IGS
Output parameters:
The clock errors of reference station ---ref_i_C(epoch,1)
Satellite elevation angle at each epoch --- ref_i_elev(epoch, sat_id)
The weight of observations --- ref_i_sat_p(epoch, sat_id)
Introduction:
This subroutine computes the clock error of reference station using Pseudorange C1 and known site coordinate.

ref_clock_2.f90

Input parameters:
Reference station ID; the structure variable IGS
Output parameters:

The tropospheric delay of reference station at every epoch ---ref_i_trop(epoch, sat_id)

ref_clock_3.f90

Input parameters:

Reference station ID; the structure variable IGS

Output parameters:

The clock errors of reference station	---ref_i_C(epoch,1)
Satellite elevation angle at each epoch	---ref_i_elev(epoch, sat_id)
The weight of observations	---ref_i_sat_p(epoch, sat_id)

Introduction:

This subroutine computes the clock error of reference station using Pseudorange C1, known site coordinate and the weight matrix of ref_clock_1 solution again.

In the same time, it deletes those satellites with the low elevation angle.

search_common_sat.f90

Input parameters:

Reference station ID; Kinematic station ID

Output parameters:

The total number of common satellites	---ref_i_tot_common_sat_num(1,1)
All common satellite IDs	---ref_i_tot_common_satnum(1,i)
The times of each satellite in view	---ref_i_start_epoch_num(sat_id,1)
The start epoch of the Kth time in view	---ref_i_start_epochnum(sat_id,k)
The end epoch of the Kth time in view	---ref_i_end_epochnum(sat_id,k)
The number of common satellites at each epoch	---ref_i_common_sat_num(epoch,1)
Common satellite IDs at each epoch	---ref_i_common_satnum(epoch,1)
Logical variable of the satellite changing	---ref_i_change_sat(epoch,1)
The number of lost satellites	---ref_i_lost_sat_num(epoch,1)
Lost satellite ID	---ref_i_lost_satnum(epoch,i)
The number of added satellites	---ref_i_add_sat_num(epoch,1)
Add satellite ID	---ref_i_add_satnum(epoch,i)
The type of satellite changing	
	0---no change
	1---lost satellite
	2---add satellite
	3---lost satellite and add satellite

Introduction:

This subroutine searches the common satellites between reference station and kinematic station. And all information of satellite's changing is saved.

det_cycle_slip.f90

Input parameters:

Reference station ID; Kinematic station ID

Output parameters:

The number of cycle slips of every satellite	---ref_i_slip_num(sat_id, k)
The epoch number of cycle slips of every satellite	---ref_i_slipnum(sat_id, k,kk)
The number of outliers of every satellite	---ref_i_outlier_num(sat_id, k)

The epoch number of outliers of every satellite ---ref_i_outliernum(sat_id, k,kk)

Introduction:

The subroutine is used to detect the cycle slip and outlier of every satellite based on the median method. And it removes those observations if the observation time is less than the minimum observation time. At the same time, the information of satellite rising and downing is updated. Additionally, the reference satellite is chosen automatically.

Note:

The reference satellite is always placed on the 1st order in HALO_GPS.

form_sd_dd.90

Input parameters:

Reference station ID; Kinematic station ID

Output parameters:

The single differenced LC observations ---ref_i_vobs8_sd(epoch,sat_id)
The double differenced LC observations ---ref_i_vobs8_dd(epoch,sat_id)
The initial double differenced ambiguity of LC observations ---ref_i_dd_amb_LC(sat_id,k)

Introduction:

The subroutine is used to compute the single and double differenced LC observations. Additionally, the initial double differenced ambiguity of L1, L2, and LC observation is fast obtained by a new method, which is introduced in Chapter 5.

a_x_l.f90

Input parameters:

Reference station ID

Output parameters:

A_row, A_rank ---the row and column of matrix_A
X_row, X_rank ---the row and column of matrix_X
L_row, L_rank ---the row and column of matrix_L
P_row, P_rank ---the row and column of matrix_P
ref_i_amb_num ---the number of ambiguity paramters
ref_i_xyz_num ---the number of position paramters
logical_amb(j,sat_id,k) ---the Kth ambiguity of ith satellite at jth epoch

Introduction:

This subroutine computes the row and column number of some important matrix, which will be used in the adjustment.

sequential_adjustment.f90

Input parameters:

Reference station ID; the structure variable IGS

Output parameters:

The final coordinate of kinematic station
---kin_i_X(epoch,1)/kin_i_Y(epoch,1)/kin_i_Z(epoch,1)
---kin_i_B(epoch,1)/kin_i_L(epoch,1)/kin_i_H(epoch,1)
The precision information at every epoch
---kin_i_sigmaX(epoch,1)/kin_i_sigmaY(epoch,1)/kin_i_sigmaZ(epoch,1)
---kin_i_sigmaB(epoch,1)/kin_i_sigmaL(epoch,1)/kin_i_sigmaH(epoch,1)

RMS at every epoch ---kin_i_RMS(epoch,1)
The final double differenced ambiguity of LC observation ---ref_i_dd_amb_LC(sat_id,k)

Introduction:

The final coordinate and ambiguities of kinematic station are calculated based on the robust sequential adjustment.

2.3 Diagram of Software

The data processing steps of this software are described in Fig.1.

(1) Program start;
(2) Read input parameter file for controlling the run of the software (an example of the definition of the input parameter file is presented in Chapter 3);
(3) Read all possible data files for the run of the software (e.g., satellite information file, station information file, tropospheric delay correction file, receiver antenna phase centre correction file, etc.);
(4) Compute all possible corrections (e.g., antenna phase centre correction, earth tide correction, tropospheric delay correction, clock error offsets, etc.);
(5) Data preprocessing (e.g., searching the common satellite, detecting cycle slip and outlier, removing bad observation and receiver clock jump, etc.);
(6) Construction of single and double differenced observations;
(7) Initialization of matrix and all unknown parameters;
(8) Parameters estimation using sequential adjustment;
(9) Robust estimation;
(10) Output the results and summary;
(11) End of Program.

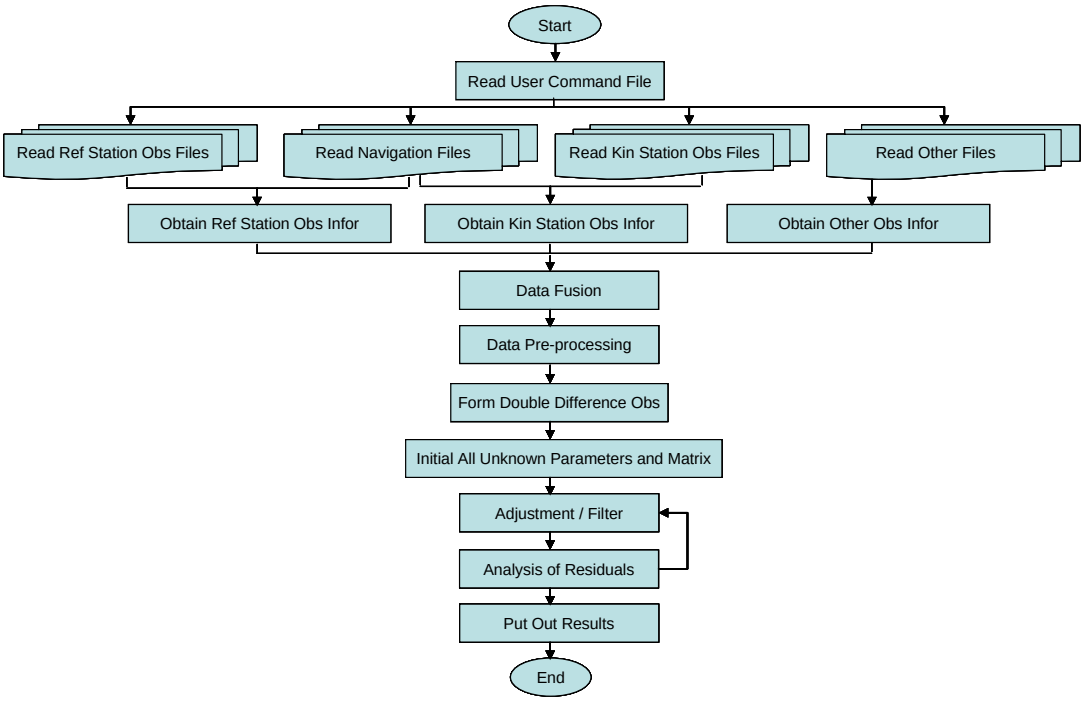

Fig.1 The data processing flowchart of HALO_GPS

3. Control File

The essential work to run the program for GPS data processing is to write an input parameter file defined in a flexible form. Definitions of the input parameters, and control file format as well as a standard control file template are introduced in following subsections.

3.1 Definitions of Input Parameters

(1) Address of precise ephemeris
---character(len=57):: address_sp3_file
(2) Address of broadcast ephemeris
---character(len=57) :: address_brdc_file
(3) Address of observation file at the 1st reference station
---character(len=57) :: address_ref_1_obsfile
(4)_(11) Address of observation file at the 2nd ~ 9th reference stations
(12) Address of observation file at the 1st kinematic station
---character(len=57) :: address_kin_1_obsfile
(13) Name of the 1st reference station
---character(len=57) :: name_ref_1
(14)_(21) Name of the 2nd ~ 9th reference stations
(22) Name of the 1st kinematic station
---character(len=57) :: name_kin_1
(23) XYZ coordinates of the 1st reference station
---real*8 X_ref_1,Y_ref_1,Z_ref_1
(24)_(31) XYZ coordinates of the 2nd ~ 9th reference stations
(32) XYZ coordinates of the 1st kinematic station
---real*8 X_kin_1,Y_kin_1,Z_kin_1
(33) The start time of data processing at the 1st reference station
---integer*4 ref_1_start_year; integer*4 ref_1_start_month;
integer*4 ref_1_start_day; integer*4 ref_1_start_hour
--- ref_1_start_min; real*8 ref_1_start_sec; real*8 ref_1_start_MJD
(34) The specified epoch number at the 1st reference station
--- integer*4 ref_1_num_epoch
(35)_(50) The start time of data processing and the solution epoch number
at the 2nd ~ 9th reference stations
(51) The start time of data processing at the 1st kinematic station
---integer*4 kin_1_start_year; integer*4 kin_1_start_month;
---integer*4 kin_1_start_day; integer*4 kin_1_start_hour
---integer*4 kin_1_start_min; real*8 kin_1_start_sec; real*8 kin_1_start_MJD
(52) The specified epoch number at the 1st kinematic station
---integer*4 kin_1_num_epoch
(53) The process strategy of ambiguity solution
---character(len=57) :: amb_pro_method

(54) The tropospheric delay file from user
---character(len=57) :: address_user_ZTD_file
(55) The ephemeris file from user
---character(len=57) :: address_user_EPH_file
(56) Satellite elevation cut off angle
---real*8 min_elev
(57) Minimum observation time
---integer*4 min_lag
(58) Adjustment method
---character(len=21) :: adjust_method
(59) Robust estimation switch
---integer*4 robust
(60) Definitions of parameters in robust estimation
---real*8 robust_k0, robust_k1
(61) The method of weight determination
---integer*4 elev_p
(62) Address of result file 1
---character(len=57) :: address_result_file_xyz
(63) Address of result file 2
---character(len=57) :: address_result_file_blh

3.2 Control File Format

The proper control file format is necessary to run HALO_GPS software. There are a total of 63 command lines in the control file. Each line includes 100 characters, where the front of 60 characters is the commands and the back 40 characters are the comments. The 1st character of each line is a switch, where 0 means close and 1 is open.

Example:

Switch	**commands (60 characters)**	**comments (40 characters)**
1	./Example/data_file/AlpinAero2008/igs14984.sp3	|Sp3 file 1

3.3 An Example of Control File

The following is an example of a standard control file for an aircraft kinematic positioning. Explanations will be outlined after this input parameter file. The control file of all other numerical tests given in this manual can be obtained through minor modification from this standard input control file.

User Control File

Created by Qianxin Wang February 2010 Technical Advisor: Tianhe Xu, Guochang Xu

---

| |

---

1. Navigation File

1|./Example/data_file/AlpinAero2008/igs14984.sp3 |Sp3 file 1

0| |Broadcast Ephemeris 2

---

2. Reference Station Observation File

1|./Example/data_file/AlpinAero2008/opaf2690.08o |1st reference station 3

0| |2nd reference station 4

0| |3rd reference station 5

0| |4th reference station 6

0| |5th reference station 7

0| |6th reference station 8

0| |7th reference station 9

0| |8th reference station 10

0| |9th reference station 11

---

3. Kinematic Station Observation File

1|./Example/data_file/AlpinAero2008/air12690.08o |1st kinematic station 12

---

4. Reference Station Name

1|OPAF |1st reference station 13

0| |2nd reference station 14

0| |3rd reference station 15

0| |4th reference station 16

0| |5th reference station 17

0| |6th reference station 18

0| |7th reference station 19

0| |8th reference station 20

0| |9th reference station 21

---

5. Kinematic Station Name

1|air1 |1st kinematic station 22

---

6. Reference Station Coordinate

X	Y	Z		
1| 4186557.029	835026.434	4723761.505	|1st reference station	23
0|			|2nd reference station	24
0|			|3rd reference station	25
0|			|4th reference station	26
0|			|5th reference station	27
0|			|6th reference station	28
0|			|7th reference station	29
0|			|8th reference station	30
0|			|9th reference station	31

---

7. Kinematic Station Coordinate

X	Y	Z		
1|0.0	|0.0	|0.0	|1st kinematic station	32

---

8. Reference Station Start Time and Epoch Number

1|2008 09 25 08 07 44.0	|1st reference station	33
1|23226	|1st reference station	34
0|	|2nd reference station	35
0|	|2nd reference station	36
0|	|3rd reference station	37
0|	|3rd reference station	38
0|	|4th reference station	39
0|	|4th reference station	40
0|	|5th reference station	41
0|	|5th reference station	42
0|	|6th reference station	43
0|	|6th reference station	44
0|	|7th reference station	45
0|	|7th reference station	46
0|	|8th reference station	47
0|	|8th reference station	48
0|	|9th reference station	49
0|	|9th reference station	50

---

9. Kinematic Station Start Time and Epoch Number

1|2008 09 25 08 07 44.0	|1st kinematic station	51
1|23226	|1st kinematic station	52

---

10. Ambiguity Strategy Used

1|float |fixed or float 53

---

11. User Troposphere File

0| |Address of User Troposphere File 54

---

12. User Ephemeris File

0| |Address of User Ephemeris File 55

---

13. Satellite Elevation Cut off Angle

1|15.0 |Satellite Elevation Cut off Angle 56

---

14. Minimum Good Observation Epochs

1|60 |Minimum Observation Epoch Number 57

---

15. Adjustment Method

1|Sequential Adjustment |Sequential or Kalman Filter 58

---

16. Robust Estimation

1|0 |1=open or 0=close 59

---

17. Robust Parameters

1|k0=1.0|k1=5.0 |k0(1.0-1.5) k1(3.0-5.0) 60

---

18. Weighted Model

1|0 |1=Elevation or 0=Equivalence 61

---

19. Result File

1|./Example/result_file/HALO_XYZ_1.txt |address of result file 62
1|./Example/result_file/HALO_BLH_1.txt |address of result file 63

---

4. File Format

4.1 Input File Format

A number of formats are currently used within the GNSS community for the exchange of data, products, and solutions. The most important and widely accepted format is the RINEX (**R**eceiver-**IN**dependent **EX**change format) used for the exchange of GNSS observations, broadcast information, and meteorological measurements. The HALO_GPS Software, Version 1.0, supports the following input file formats:

RINEX for the exchange of observation data, broadcast information, and meteorological data,

SP3 for the exchange of precise orbit and satellite clock information,

Troposphere SINEX (**S**olution-**IN**dependent **EX**change format) for the export of troposphere information,

Clock RINEX for the exchange of satellite and receiver clock information.

4.2 Output File Format

For ease of use the products and solutions of this software, the output file format of HALO_GPS is introduced below.

(1). The positioning results in Geodetic coordinates system:

```
          1         2         3         4         5         6         7         8         9         0         1
1234567890123456789012345678901234567890123456789012345678901234567890123456789012345678901234567890123456789
2007  6  7  6 55  11.000  55.52214972   8.54791440  70.438   0.002   0.002   0.004   0.005
2007  6  7  6 55  12.000  55.52214978   8.54791436  70.437   0.004   0.003   0.007   0.008
2007  6  7  6 55  13.000  55.52214976   8.54791445  70.448   0.006   0.004   0.010   0.013
2007  6  7  6 55  14.000  55.52214983   8.54791430  70.433   0.016   0.012   0.030   0.036
2007  6  7  6 55  15.000  55.52214978   8.54791434  70.438   0.004   0.003   0.007   0.008
Year  M Day H Min Second   Latitude      Longitude    Height  sigma(B) sigma(L) sigma(H) RMS(Total)
```

(2). The positioning results in Cartesian coordinates system.

Ep	Y	M	D	H	M	Second	X	dX	Y	dY	Z	dZ	RMS	DD
1	2010	1	2	0	0	0.00	-2399062.732	0.010	5389237.877	0.026	2417327.081	0.016	0.032	7
2	2010	1	2	0	0	5.00	-2399062.733	0.009	5389237.870	0.023	2417327.075	0.014	0.029	7
3	2010	1	2	0	0	10.00	-2399062.733	0.011	5389237.874	0.029	2417327.087	0.018	0.036	7
4	2010	1	2	0	0	15.00	-2399062.735	0.009	5389237.876	0.023	2417327.082	0.014	0.028	7
5	2010	1	2	0	0	20.00	-2399062.731	0.010	5389237.875	0.025	2417327.080	0.015	0.031	7

5. Strategies and Principles

The HALO_GPS is developed to fulfill the needs of German HALO (**H**igh **A**ltitude and **LO**ng Range Research Aircraft) project. The main strengths of the proposed HALO aircraft are its long range (about 10000 km) and endurance (more than 10 flight hours), high ceiling altitude (more than 15 km) and large instrument load capacities, which are not available in such combination on any other research aircraft in Europe. Therefore, it brings many new challenges for airborne GPS kinematic positioning. In order to obtain a precise aircraft trajectory, some new strategies and techniques are developed in HALO_GPS. Although these methods are introduced in the references, the theories will be described briefly.

5.1 Outlier and Cycle Slip Detection

An ambiguity break, a so-called cycle slip, occurs when the phase observation jumps by a few or more cycles in L1 frequency, L2 frequency, or in both. A single outlier is defined as an isolated shift of observation which lasts only one or a few epochs whereas a cycle slip causes a systematic constant shift in the observation. The variation of position with time in a kinematic survey makes it hard to use a single observation for the detection of the cycle slips. In a static GPS analysis, it is possible to scan the pre-processed residuals with a priori model for data quality control and to detect potential cycle slips at any epoch. In a kinematic survey, the pre-fit residuals are of little use because of the movement of one receiver. We use the two geometry-free linear combinations of phase data: the W-M widelane (L6) and the extra-widelane (L4) to detect potential cycle slips and outliers. The calculate formula of L4 and L6 are as follows:

$$L4 = \varphi_1 - \frac{\lambda_2}{\lambda_1}\varphi_2 = N_1 - \frac{\lambda_2}{\lambda_1}N_2 - \frac{\kappa}{c\lambda_1}\left(\frac{1}{f_1^2} - \frac{1}{f_2^2}\right) \tag{1}$$

$$L6 = \varphi_1 - \varphi_2 - \frac{f_1 - f_2}{f_1 + f_2}\left(\frac{P_1}{\lambda_1} + \frac{P_2}{\lambda_2}\right) = N_1 - N_2 \tag{2}$$

where φ_1, φ_2, P_1, P_2, N_1, N_2, f_1, f_2 are the phase observations, the pseudorange observations, the ambiguities and the frequencies in L1 and L2, respectively. κ is ionospheric delay and c is the speed of light.

The right-hand side of Eq. (1) shows that the residual contains only the L1 and L2 ambiguities and ionospheric delay. Moreover, the contribution of ionosphere is reduced by 65% by the factor $\left(\frac{1}{f_1^2} - \frac{1}{f_2^2}\right)$.

We re-write Eq. (1) as

$$N_1 - \frac{\lambda_2}{\lambda_1}N_2 = L4 + \frac{\kappa}{c\lambda_1}\left(\frac{1}{f_1^2} - \frac{1}{f_2^2}\right) \tag{3}$$

Eq. (3) denotes the frequency relationship directly and exclusively between the L1 and L2 ambiguity for each satellite from the phase observations. If there were no cycle slips, the temporal variations of the ionospheric residual in Eq. (3) would be small for normal ionospheric conditions. Thus this combination of ambiguities will be close to constant. In our experiment, the average variation size of the extra-widelane ambiguities is around 0.02 to 0.2 cycles for most of satellites.

For the same reason, W-M combination can be applied, which introduces noise from pseudorange measurements but eliminates ionospheric effects. The RMS of widelane ambiguity in Eq. (2) is usually 0.2 ~ 0.5 cycles.

The treatment of the cycle slips includes two steps: detection and fixing. Firstly, we examine the ambiguity N6 of widelane L6 and ambiguity N4 of extra-widelane L4. The widelane ambiguity N6 is ionosphere free and suffers only from system measurement noise and multipath variations. Also the ionospheric effects are largely reduced in L4. Such errors should be smooth over several epochs compared to a cycle break. When a discontinuity occurs in the widelane, there is a possible cycle break there. Then we decide these doubtful cycle slips based on a statistical test model. The median method is used to avoid the detection is broken down by some too larger abnormal observations.

5.2 Clock Error Estimation

The clock error is one of the major errors in GPS surveying. A small clock error may cause a very large code and phase error. Therefore, we have to carefully model the clock error on the satellites and receiver. We use IGS precise ephemeris to obtain the precise satellite clock corrections (the precision is better than 0.1 nanoseconds). Meanwhile, the receiver clock error is estimated together with other parameters in station coordinate estimation. In order to avoid the excess parameters, a white noise model is usually used to express the behavior of receiver clock errors.

5.3 Tropospheric Delay Correction

A regional tropospheric model can be constructed using surveys from GPS ground networks. Using this model the tropospheric delays of a kinematic station within the region can be interpolated. However, such a model is generally not suitable for an airborne platform high above the ground networks. Therefore, a method of constructing a regional tropospheric model for airborne GPS applications is developed and used in HALO_GPS. First, the kinematic station in the air is projected onto the ground. Then the tropospheric delays at projected point are interpolated from those of the ground networks. Finally, the tropospheric delays at projected point are extended upward to the airborne platform using pressure and temperature gradients and humidity exponential function. This method is called “Projection Extension Method” (PEM) for convenience of later discussion.

To investigate the impact of different tropospheric delays on GPS kinematic positioning, some experiments were performed. An IGS site (site name: OBE3) is taken as a fixed site; a SAPOS site (site name: ZUGS) is treated as a kinematic station to estimate its coordinates at every epoch. The tropospheric delays are obtained from remove-restore method (RRM) and PEM, respectively. The observation time is from 00:00:00 to 06:59:59 on 17th Dec. 2008. GAMIT daily solution is regarded as reference values. Fig. 2 and Fig. 3 show the residuals of tropospheric delays and the residuals of estimated elevations using RRM and PEM, respectively. Table 1 presents statistical results of kinematic positioning precision.

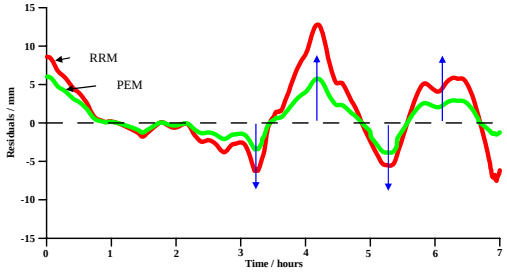

Fig. 2 The residuals of tropospheric delays using RRM and PEM

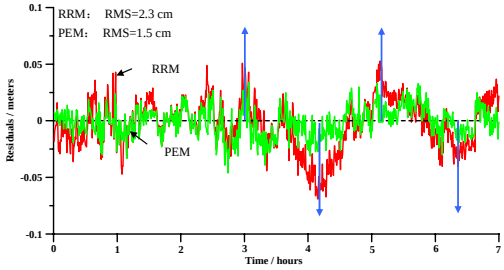

Fig. 3 The residuals in height component using RRM and PEM

Table 1 Comparison of the precision of GPS kinematic positioning using RRM and PEM (unit: cm)

Method	L	B	H
RRM(rms)	0.83	1.37	2.32
PEM(rms)	0.85	1.34	1.51

Fig. 2 and Fig. 3 show a negative correlation between ZTDs and the elevation. When the estimated ZTDs are larger than the true ZTDs, the estimated elevation will be smaller than the true elevation; when the estimated ZTDs are smaller than the true ZTDs, the estimated elevation will be larger than the true elevation. From Table 1, the positioning precisions on two horizontal components are similar using RRM and PEM. However, the positioning precision in height component of PEM is 8 mm better than that of RRM. In some applications, e.g. airborne gravity determination, it is just the height component, which is of ultimate importance.

5.4 Ambiguity Resolution

Unlike other factors which have common sources, the phase bias is receiver channel dependent. In GPS receiver, each channel initializes its own counter for one satellite so the phase biases can not be canceled by differencing and modeling. Resolving unknown phase bias becomes a fundamental requirement for accurate cm-level GPS aircraft kinematic positioning.

Moreover, ambiguity resolution is more crucial in the kinematic surveying than in the static one. In static GPS analysis, we can separate the ambiguities from the receiver's fixed position by the geometric changes of satellite in a long time observation. In kinematic GPS surveying, the occupation of receiver in one location is short, even varies from epoch by epoch. The ambiguities are high-correlated with positions. Therefore, we feel the strong need to develop an ambiguity resolution method for aircraft positioning to be not only fast but also reliable – having the capability to deal with complex environmental conditions.

There is not a simple way to develop a comprehensive approach for ambiguity solution considering the complex field conditions in which GPS surveys performed. In HALO_GPS software, an ambiguity search in the ambiguity space is done and includes the following five steps:

1、 Selection of an initial search center

2、 Selection of a search space

3、 Reduction of search candidates by the constraint conditions of geometry and physics

4、 Searching for the best candidates

5、 Significance check and verification

The initial ambiguities are obtained by the following equations:

$$\nabla\Delta N_{L1} = \frac{\nabla\Delta N_{L4} \times \lambda_1 - \nabla\Delta N_{L6} \times \lambda_2}{\lambda_1 - \lambda_2} \tag{4}$$

$$\nabla\Delta N_{L2} = \frac{\nabla\Delta N_{L4} \times \lambda_1 - \nabla\Delta N_{L6} \times \lambda_1}{\lambda_1 - \lambda_2} \tag{5}$$

$$\nabla\Delta N_{LC} = \frac{f_1^2}{f_1^2 - f_2^2}(\nabla\Delta N_{L1} - \frac{f_2}{f_1} \times \nabla\Delta N_{L2}) \tag{6}$$

where $\nabla\Delta N_{L4}, \nabla\Delta N_{L6}$ is the double differenced ambiguities of the extra-widelane (L4) and the W-M widelane (L6). The $\nabla\Delta N_{L4}, \nabla\Delta N_{L6}$ can be obtained by the Eq. (2), (3). The detailed introduction of this method is given in the references.

5.5 Robust Estimation

Since the precision of GPS phase observations are better than 1 mm, it is usually used for the precise positioning. However, there inevitably exist observational outliers in the real surveying. If the outliers are not eliminated or controlled, the estimated parameters will be distorted. There are two commonly used methods to control the outliers. One is the outlier detection, which detects the outliers by statistic test. Since this method is usually based on the least squares (LS) adjustment, the statistic will be influenced by the outliers. The other is robust estimation, which controls the effect of outliers by the equivalent weight. When there are anomalies both in the prior parameters and the measurement data, it may lead to divergence of the solution.

In order to controlling the influences of the outliers, the combination of outlier detection and robust estimation is adopted in HALO_GPS. Firstly, the large outliers are detected and moved out based on the median method in the data preprocessing. Then, the residual outliers are controlled by the robust estimation in the parameter adjustment. The IGG3 scheme is applied to determine the equivalent weight. The calculation formula of the equivalent weight is given below:

$$\overline{P} = \gamma P \tag{7}$$

where $\overline{P}$ is the equivalent weight; P is the original weight; γ is the adjusting factor of weight. And the factor γ is decided by the following formula:

$$\gamma = \begin{cases} 1 & \bar{v} \le k_0 \\ \dfrac{k_0}{|\bar{v}|}\left(\dfrac{k_1 - |\bar{v}|}{k_1 - k_0}\right)^2 & k_0 < \bar{v} \le k_1 \\ 0 & \bar{v} > k_1 \end{cases} \tag{8}$$

where $\bar{v}$ is the standardized residual; the value range of k_0 is usually from 1.0 to 1.5; k_1 is from 3.0 to 5.0.

5.6 Adjustment Method

There are numerous adjustment methods that can be used, but least squares (LS) adjustment is the simplest and basic one. For static case the LS adjustment algorithm is directly used for determining the complete unknowns. For kinematic case, there are two groups of unknowns. One change with the time (e.g. coordinates) and another does not (e.g. ambiguities). A sequential adjustment algorithm is especially suitable for kinematic case to separate the time dependent unknowns and time independent unknowns, so one can solve for position every epoch in one hand, and obtain the updated ambiguity information for further use in the other hand. The estimated coordinate will be improved as the ambiguity information accumulated. The best ambiguity solution will be obtained when the whole observations involved, so a repeat computation of the kinematic coordinates by using the best known ambiguity is necessary for the homogeneous coordinate solutions.

5.7 Automatic Choosing and Changing Reference Satellite

In the long time GPS surveying, changing reference satellite is inevitable. Therefore, we develop an efficient method to deal with this problem. It is introduced below.

The relationship between un-differenced ambiguity and double differenced ambiguity before changing reference satellite can be expressed as:

$$\nabla\Delta N = AN_0 \tag{9}$$

And the relationship between un-differenced ambiguity and double differenced ambiguity after changing reference satellite can be expressed as:

$$\nabla\Delta\overline{N} = BN_0 \tag{10}$$

where $\nabla\Delta N$, $\nabla\Delta\overline{N}$ are the old and new double differenced ambiguity, respectively; A, B are the transformed matrix; N_0 is un-differenced ambiguity.

The relationship between the new double differenced ambiguity and the old double differenced ambiguity can be assumed as:

$$\nabla\Delta\overline{N} = C\nabla\Delta N \tag{11}$$

Therefore, it is key problem that how to get the matrix C. Through some matrix transformations, we get the general form of factor matrix C:

$$C = BA^T(AA^T)^{-1} \tag{12}$$

Finally, the new double differenced ambiguity $\nabla\Delta\overline{N}$ is easy to be obtained by the old double differenced ambiguity $\nabla\Delta N$ multiplied by the matrix C.

5.8 Automatic Choosing and Changing Reference Station

This function is specially developed for HALO project. Although the principle and method are

introduced systematically in our publications, the theories will be described briefly here.
The single baseline model is the simplest and commonly used model in kinematic relative positioning. However, such a model is generally not suitable for the long range flight positioning. Due to the long distance between reference station and kinematic station, many kinds of common errors can not be cancelled out by the difference method. And the number of common satellites will be decreased with the increase of baseline length. If a closer reference station can be used in place of the original reference station, these problems will be solved well. Therefore, a method of adaptively changing reference station for long distance airborne GPS applications is developed in HALO_GPS software. The basic idea is that the positioning model always keeps the single baseline model during the whole solution. When the distance between kinematic station and reference station is longer than the maximum distance which is defined by user, the new reference station will used to replace the old one. At the same time, all information of old observation equation including covariance matrix are transferred to the new observation equation based on the equivalent eliminated parameter method. The calculation steps of adaptively changing reference station are described below.

Firstly, we suppose that the observation equation before changing reference station can be written as:

$$L - A\begin{bmatrix} X_1 \\ X_2 \\ \nabla\Delta N_{i1,i2} \end{bmatrix} = V, \quad P \tag{13}$$

And the observation equation after changing reference station can be expressed as:

$$L' - B\begin{bmatrix} X_1' \\ X_2' \\ \nabla\Delta N_{i3,i2} \end{bmatrix} = V', \quad P' \tag{14}$$

where L, L' are the observations; A, B are the design matrices; X_1, X_2, X_1', X_2' are the position parameters; $\nabla\Delta N_{i1,i2}, \nabla\Delta N_{i3,i2}$ are the double differenced ambiguities between old reference station $i1$ and kinematic station $i2$, and those of new reference station $i3$ and kinematic station $i2$, respectively; V, V', P, P' are the residual vectors and the weight matrices, respectively. It is to be noted that X_2, X_1' are the same position parameters of kinematic station.
Then, the Eq. (13) can be rewritten as:

$$L - \begin{bmatrix} A_1 & A_2 \end{bmatrix}\begin{bmatrix} X_2 \\ \overline{X} \end{bmatrix} = V, \quad P \tag{15}$$

where $\overline{X}$ includes X_1 and $\nabla\Delta N_{i1,i2}$.
Normal equation of Eq. (15) can be obtained as:

$$\begin{bmatrix} M_{11} & M_{12} \\ M_{21} & M_{22} \end{bmatrix}\begin{bmatrix} X_2 \\ \overline{X} \end{bmatrix} = \begin{bmatrix} U_1 \\ U_2 \end{bmatrix} \tag{16}$$

where

$$\begin{bmatrix} M_{11} & M_{12} \\ M_{21} & M_{22} \end{bmatrix} = \begin{bmatrix} A_1^T PA_1 & A_1^T PA_2 \\ A_2^T PA_1 & A_2^T PA_2 \end{bmatrix} \tag{17}$$

$$\begin{bmatrix} U_1 \\ U_2 \end{bmatrix} = \begin{bmatrix} A_1^T PL \\ A_2^T PL \end{bmatrix} \tag{18}$$

The two sides of Eq. (16) are multiplied by the matrix K,

where

$$K = \begin{bmatrix} E & -Z \\ 0 & E \end{bmatrix} \tag{19}$$

E is a unit matrix; $Z = M_{12}M_{22}^{-1}$.

Then the Eq. (16) can be transformed as:

$$\begin{bmatrix} M_1 & 0 \\ M_{21} & M_{22} \end{bmatrix} \begin{bmatrix} X_2 \\ \overline{X} \end{bmatrix} = \begin{bmatrix} R_1 \\ U_2 \end{bmatrix} \tag{20}$$

where

$$M_1 = M_{11} - M_{12}M_{22}^{-1}M_{21} = A_1^T P(E - A_2 M_{22}^{-1} A_2^T P)A_1 \tag{21}$$

$$R_1 = U_1 - M_{12}M_{22}^{-1}U_2 = A_1^T P(E - A_2 M_{22}^{-1} A_2^T P)L \tag{22}$$

The Eq. (20) can be divided into two parts:

$$M_1 X_2 = R_1 \tag{23}$$

$$M_{21} X_2 + M_{22}\overline{X} = U_2 \tag{24}$$

Making $J = A_2 M_{22}^{-1} A_2^T P$ and considering $(E-J) = (E-J)(E-J)$, $P(E-J) = (E-J)^T P$ then the Eq. (21) and (22) can be expressed as:

$$M_1 = A_1^T P(E-J)A_1 = A_1^T P(E-J)(E-J)A_1 = A_1^T (E-J)^T P(E-J)A_1 \tag{25}$$

$$R_1 = A_1^T P(E-J)L = A_1^T (E-J)^T PL \tag{26}$$

Assuming $D_1 = (E-J)A_1$, the Eq. (23) can be written as:

$$D_1^T PD_1 X_2 = D_1^T PL \tag{27}$$

The equivalent observation equation of Eq. (27) is:

$$L - D_1 X_2 = V, \quad P \tag{28}$$

It is obvious that Eq. (27) and Eq. (13) are equivalent. The solutions of them are identical.

The normal equation of Eq. (14) can be written as:

$$B^T P' B \begin{bmatrix} X_1' \\ X_2' \\ \nabla\Delta N_{i3,i2} \end{bmatrix} = B^T P' L' \tag{29}$$

Since there are the same unknowns X_2, X_1' between two equations, the Eq. (27) can be added to the Eq. (29) and then get:

$$\overline{B}^{T}\overline{P}^{'}\overline{B}\begin{bmatrix} X_1^{'} \\ X_2^{'} \\ \nabla\Delta N_{i3,i1} \end{bmatrix} = \overline{B}^{T}\overline{P}^{'}\overline{L}^{'} \tag{30}$$

where $\overline{B}$, $\overline{\mathrm{L}}^{'}$ are the design matrix and observation matrix after stacking, respectively; $\overline{P}^{'}$ is the weight matrix.

Finally, the position parameters and ambiguity parameters of kinematic station can be estimated based on the Eq. (30).

6. Run of HALO_GPS

To start the HALO_GPS, the user just needs to enter the following command lines:
./ HALO
Then the following information will be shown on the user screen:

```
     HALO_GPS - High Altitude and Long Range Airborne GPS Positioning Software

  Created Date : March 2010
  Created By   : Qianxin Wang
  Advisors     : Dr. Tianhe Xu, Dr. Guochang Xu
  Email        : kingsen@gfz-potsdam.de
  Telephone    : 0049-331-288-1187
  Copyright    : Helmholtz Centre Potsdam
                 German Research Centre for Geosciences
  Version      : 1.0
 ------------------------------------------------------------------------------

                        A.  Reading Control File
 ------------------------------------------------------------------------------

Please Choose:
1 --> Run Example
2 --> Run Special Control File
3 --> Exit
```

To testing the installation of HALO_GPS software, we provide three examples to user. If the user enters 1, the program will run the examples automatically. If the user chooses 2, the address of special control file will be asked to input. The control file consist all necessary information and control parameters for running this software. And the user control file has to be edited before running the program. The format and definitions of user's own control file have been introduced in Chapter 3.

The whole data processing is automatic. After all data is processed successfully, the program will give the following information:

```
 ------------------------
 Sat: 23
 ------------------------
 Period      dd_amb_LC     Epoch
   1            28.522  2590  3000
 ------------------------
 Sat: 28
 ------------------------
 Period      dd_amb_LC     Epoch
   1             8.703     1  3000
 ------------------------
 Sat: 32
 ------------------------
 Period      dd_amb_LC     Epoch
   1            51.961     1  2218

------------------------------------------------------------------------------
Successful Solution!
Do You Want to Process Other GPS Data ?
1--->Yes
2--->No
```

If user chooses "1", the other data will be processed; otherwise the program will exited.

7. Numerical Examples

For test run of the HALO_GPS, a number of experiments have been performed. In this Chapter, some experimental results and analysis are given.

7.1 Static Data Kinematic Processing

In this experiment, the GPS data of two fixed stations are used, which are measured on February 1st 2010 at Hong Kong. One site is taken as a reference station (site name: HKST); the other site is treated as a kinematic station to estimate its coordinates at every epoch (site name: HKLT), see Fig. 4.

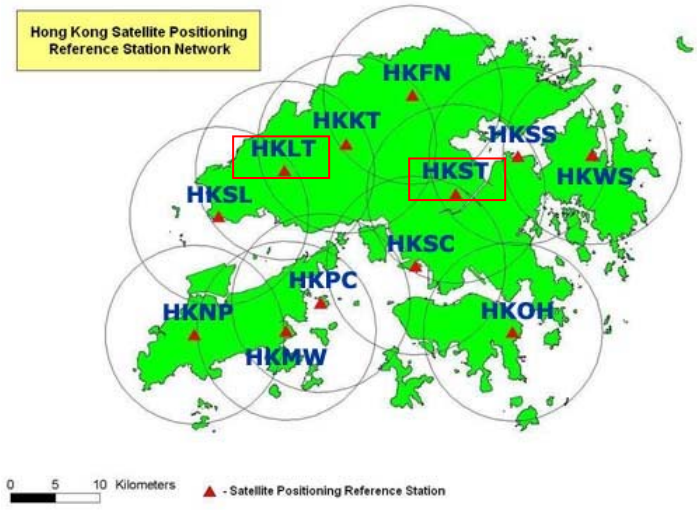

Fig. 4 Used Hong Kong GPS station network

The sampling interval of observation data is 5 seconds. 23 hours data were processed by HALO_GPS and the initial positions of HKLT are $X = 0$, $Y = 0$, $Z = 0$, without any a priori information. The positioning results are shown below.

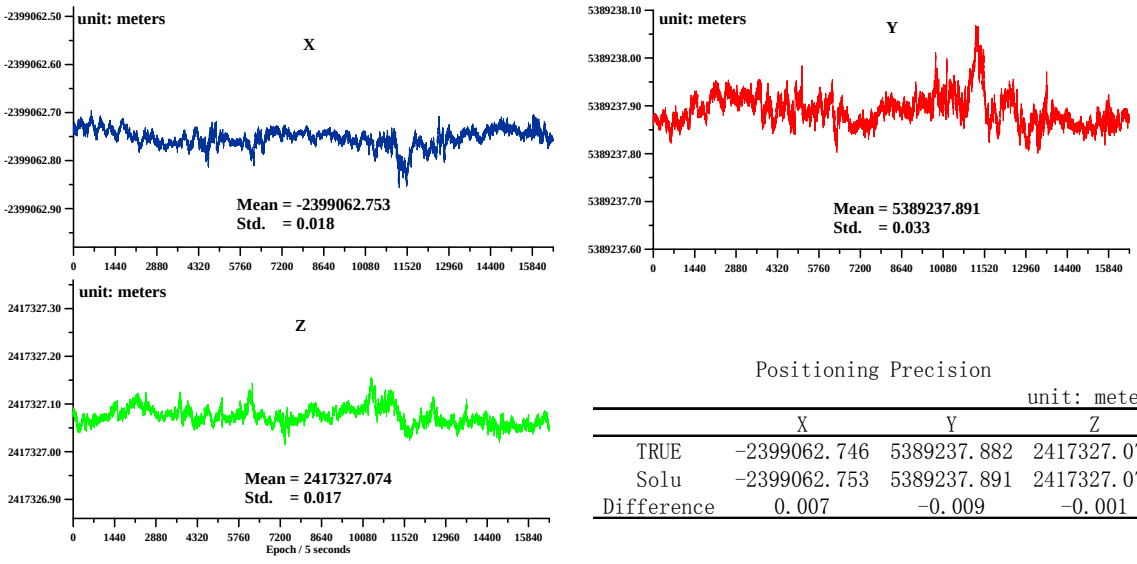

Positioning Precision

unit: meters

	X	Y	Z
TRUE	-2399062.746	5389237.882	2417327.073
Solu	-2399062.753	5389237.891	2417327.074
Difference	0.007	-0.009	-0.001

Fig. 5 The results of static station kinematic processing

Fig.5 shows the differences are the mm-level between the means of HALO_GPS and the “true” values of IGS daily solution in X Y Z three components. And the standard deviations are 1~3 cm.

7.2 Antenna Movement Experiment

For testing the capability of processing kinematic data, the antenna movement experiment is carried out on the roof of building A17 located at GeoForschungsZentrum on February 19th 2010. One is vertical motion test. In this test, the IGS reference station of GFZ is taken as the fixed station. And another GPS station is treated as the kinematic station nearby this IGS reference station, which is set up by the Department 1.1 of GFZ, see Fig. 6.

Fig. 6 Used IGS reference station and kinematic station at GFZ

The initial antenna height of kinematic station was 22.5 cm. After half an hour, the antenna height was increased to 41.5 cm, see Fig. 7. Then we use HALO_GPS software to process these data during the antenna moving. Fig. 8 shows the positioning results of HALO_GPS. The calculation results agree well with the true increments of antenna.

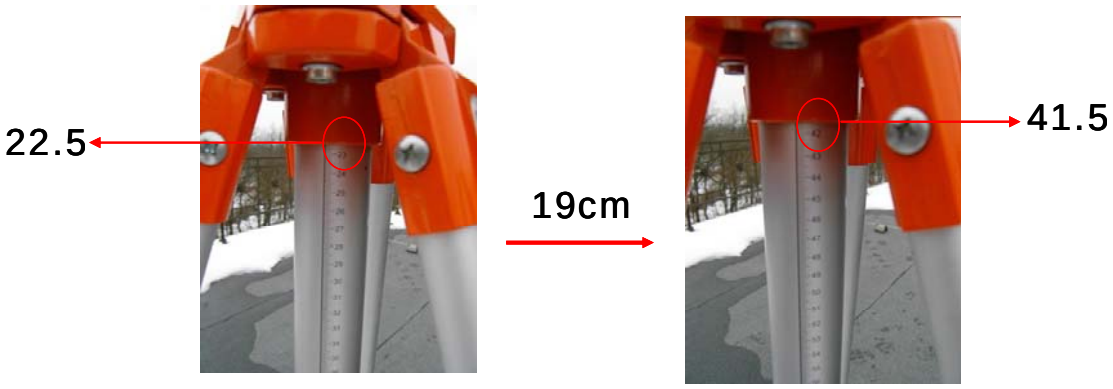

Fig.7 The vertical motion experiment

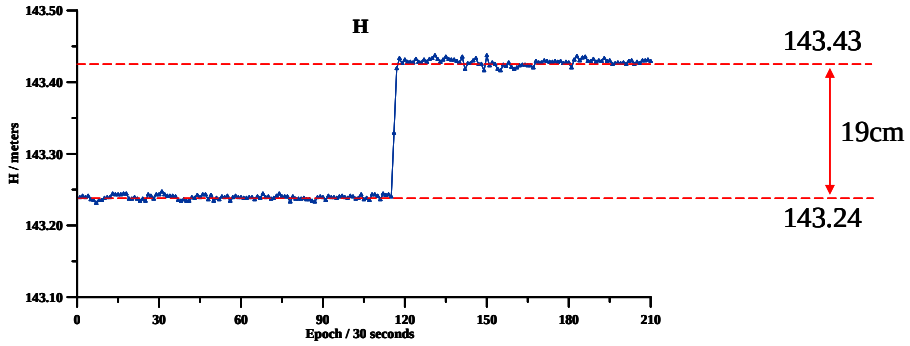

Fig.8 The positioning results on the height component

Another is horizontal motion test. Similarly, the IGS reference station of GFZ is taken as the fixed station. But the antenna of kinematic station is placed on a rule. The initial location of antenna on the rule was 103 cm. After half an hour, the antenna was moved to 43 cm on the rule, see Fig. 9. Fig. 10 shows the positioning results of HALO_GPS.

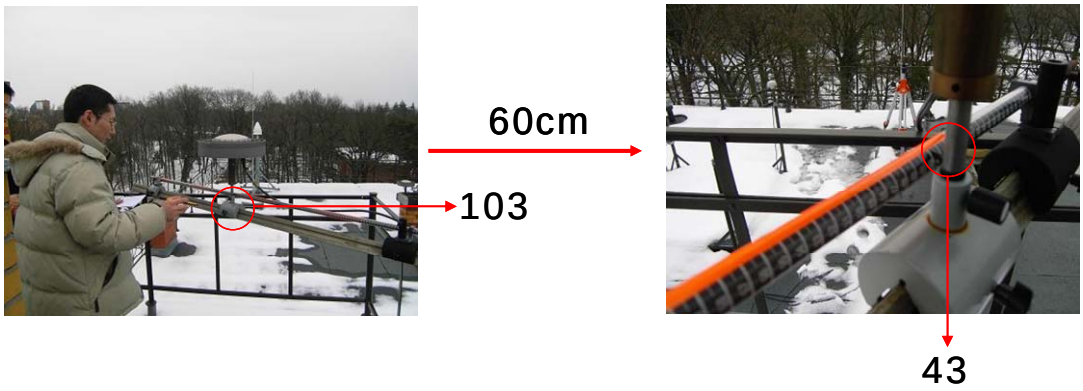

Fig.9 The horizontal motion experiment

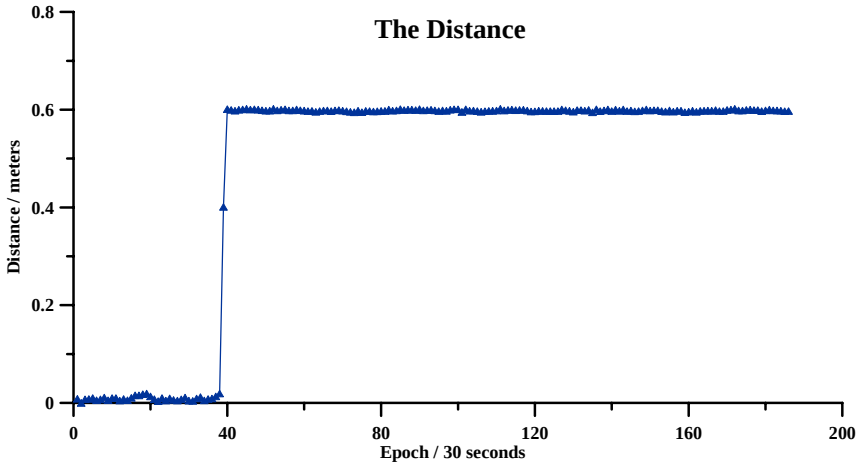

Fig.10 The positioning results of motion distance on the horizontal component

Fig.10 shows the calculation results agree well with the true distance of antenna moving.

7.3 Sea Buoy Experiment

This experiment was performed by Hong Kong Polytechnic University on December 8th 2004 at Repulse Bay, Hong Kong Island. Two Leica dual frequency GPS receivers were used, one is set on shore as a fixed station and another receiver is installed on a buoy in the sea, see Fig. 11.

Firstly we estimate the position of GPS buoy using a well known GPS commercial software Ashtech Solutions 2.60. Since the reference station is very close to the GPS buoy (about 150 meters), most GPS measurement errors can be cancelled out by the relative position mode. Therefore, the position accuracy of centimeter level can be easily achieved for this experiment. Fig. 12 is a comparison of the positioning results between HALO_GPS and Ashtech Solutions on the horizontal and height components.

Fig.11 Sea buoy experiment at Repulse Bay

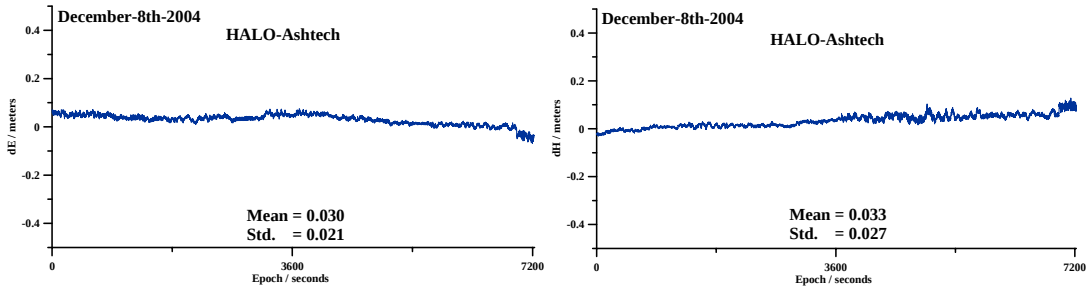

Fig.12 The comparison of the positioning results between HALO_GPS and Ashtech Solutions

Fig. 12 shows the differences between HALO_GPS and Ashtech Solution are very flat. The means and standard deviations are 2~3 cm.

7.4 NorthGrace2007 Campaign

Since HALO_GPS is developed to fulfill the need of precise positioning in airborne gravimetry, it has to be rigorously tested with real aircraft GPS data. We used it to process the GPS data of

NorthGrace2007 and AlpinAero2008 airborne gravimetry campaign. And the internal tests and external comparisons are also made.

Fig. 13 shows the plane trajectory of airplane in the NorthGrace2007 campaign. This campaign includes a total of 25 flights. The positioning results of two flights (on June 10th 2007 and June 14th 2007) are shown here. Fig. 14 is the comparisons between HALO_GPS and GAMIT on the height component.

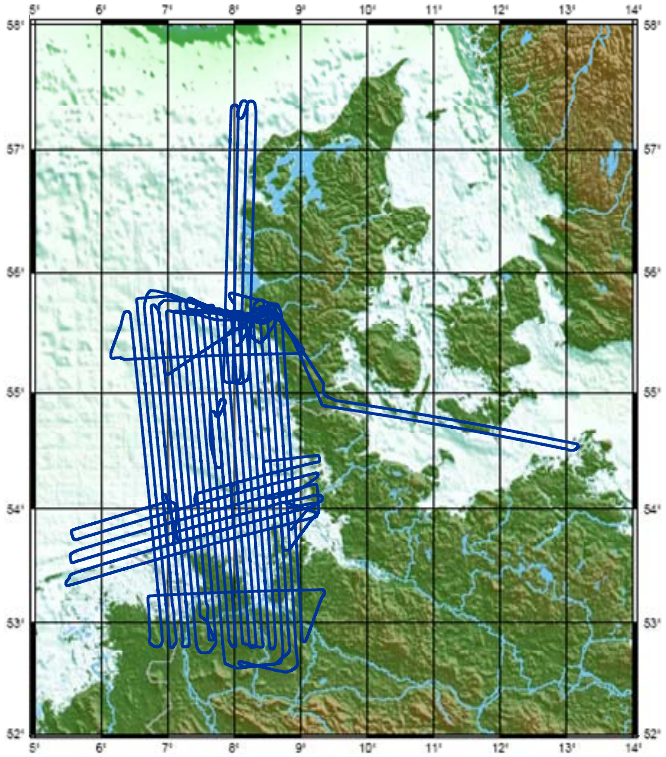

Fig.13 The plane trajectory of 25 flights in NorthGrace2007 campaign

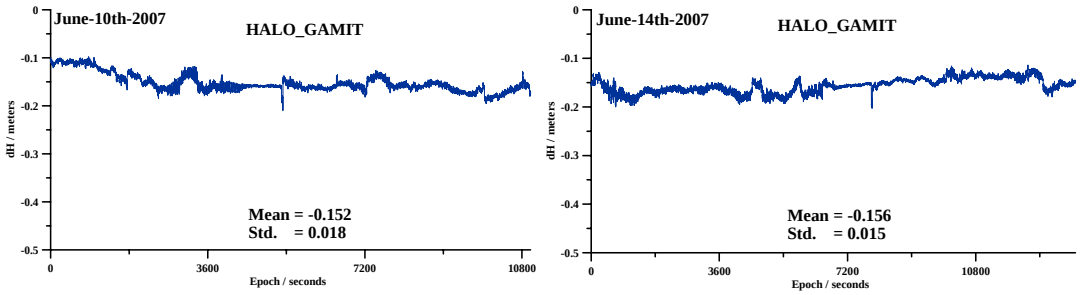

Fig. 14 The comparison of the positioning results between HALO_GPS and GAMIT

Fig.14 shows there is a 15 cm bias between the positioning results of HALO_GPS and that of GAMIT. The reason may be that the different error correction models are used in the different software. However, the standard deviations are better than 2 cm. The results are satisfied.

7.5 AlpinAero2008 Campaign

The AlpinAero2008 was an airborne survey in the Alps and their German forelands carried out by

BKG in cooperation with the GFZ (Potsdam) and BGR (Hanover) in September/October 2008 using a Beech QueenAir 88 aircraft, see Fig. 15. Fig. 17 shows the plane trajectory of 20 flights in this campaign. For geodetic positioning of the aircraft one Novatel OEM-4 and one Topcon NET-G3 GPS receivers together with a GPS-controlled inertial measurement unit Aerocontrol IIb of IGI Company were used. Data sampling rate was 10 Hz. The two GPS antennas were located at the nose and near to the tail of the aircraft, respectively (see Fig. 16). The Euclidian distance between the antennas was 5.343 meters.

For evolution of HALO_GPS, a number of internal and external comparisons are performed. Fig. 18 shows the distance variation between two GPS antennas on October 13th 2008. The distance is obtained by calculating the separate positioning results of two antennas without any a priori information. Fig. 19 is a comparison of the positioning results between HALO_GPS and GAMIT software on the height component. The flights are on September 26th 2008 and October 13th 2008, respectively. Fig. 20 is a comparison between HALO_GPS and commercial software Trimble Geomatics Office ™ (TGO) at the same days. Comparisons show good performance of HALO_GPS. The standard deviation is better than 5 cm.

Fig. 15 Beech QueenAir 88 aircraft

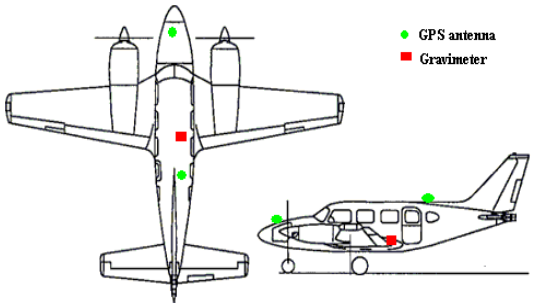

Fig. 16 Location of mounted sensors on the aircraft

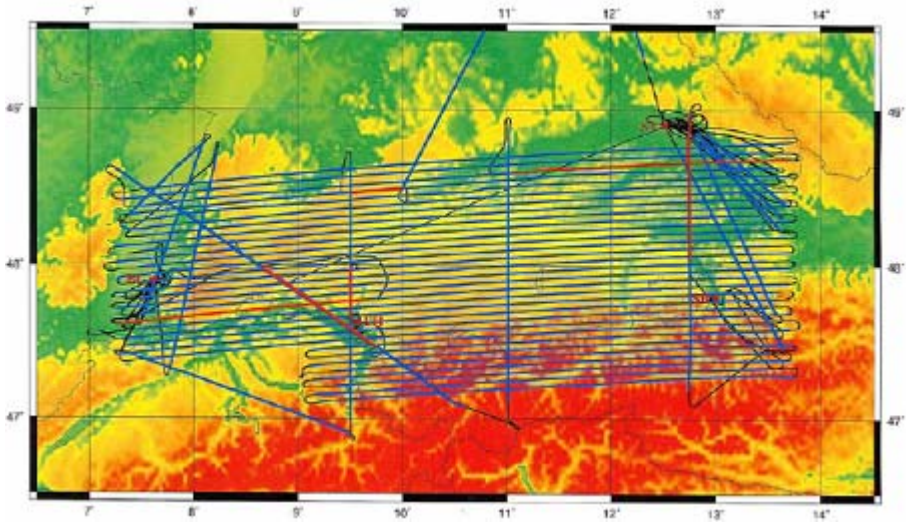

Fig.17 The plane trajectory of 20 flights in AlpinAero2008 campaign

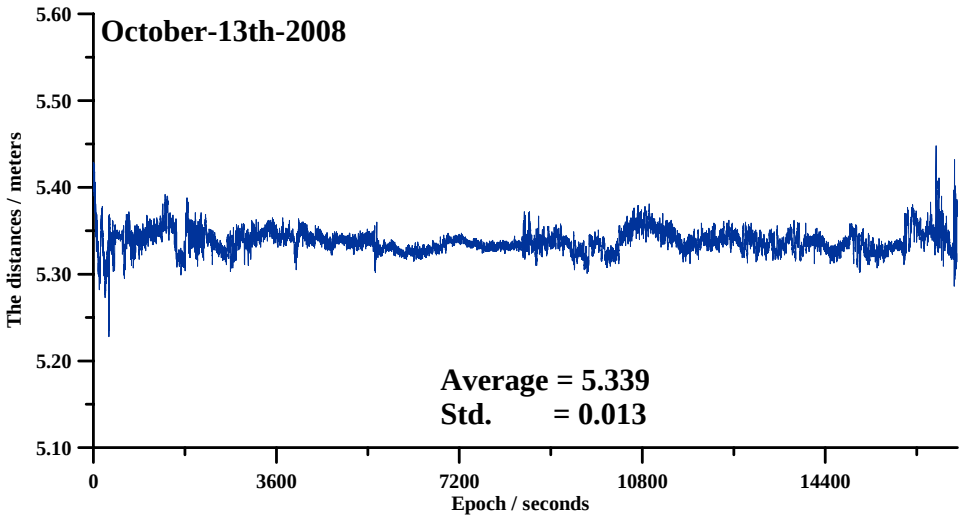

Fig. 18 The distance variation between two GPS antennas

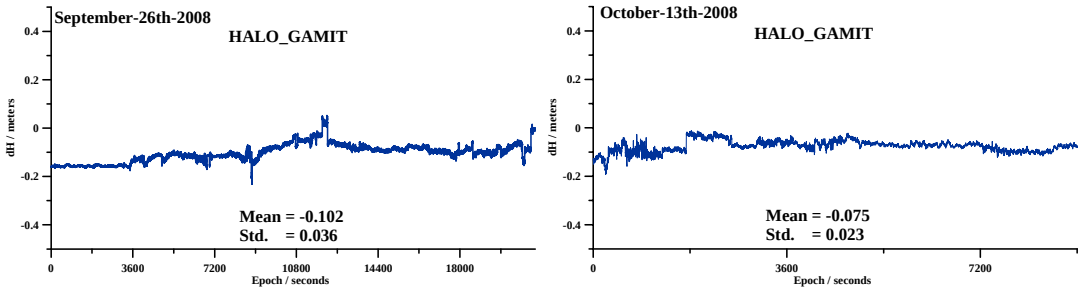

Fig.19 The comparison of the positioning results between HALO_GPS and GAMIT

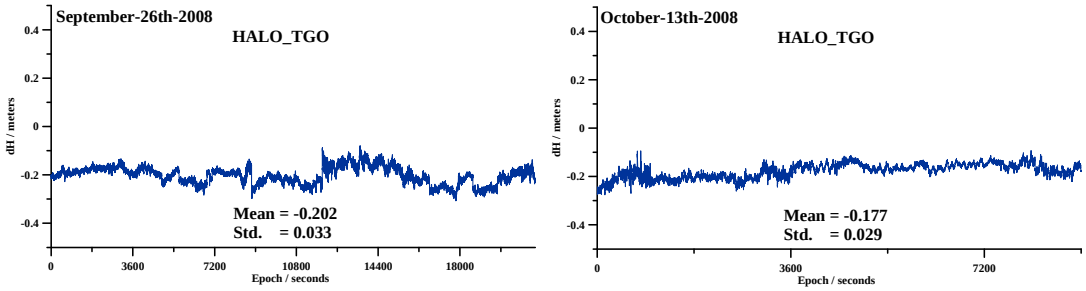

Fig.20 The comparison of the positioning results between HALO_GPS and TGO

8. Summary

HALO_GPS is developed at GFZ to achieve cm-level accuracy for an aircraft trajectory for application in airborne gravimetry. Some new strategies and algorithms are adopted to deal with complex environmental conditions in aircraft positioning, such as robust estimation, median method, and fast ambiguity resolution. Furthermore, we developed the methods of automatically choosing and changing reference satellite and the reference station to fulfill the needs of HALO project.

This software has been tested with many kinds of real data. Comparisons have been made with several well known GPS software packages. The results show the kinematic positioning accuracy of HALO_GPS is about 2 cm ~ 5 cm. Of course, any GPS software can not obtain a satisfying result, when the data quality is too bad in very few epochs. Through processing a number of real data from NorthGrace2007 and AlpinAero2008 campaign, the stability and reliability of this software are validated.

For the beginner, the one-click functionality is implemented for ease of use. All process steps will be finished automatically after the user enters one command. The application programming interface (API) is also provided for the professional users to develop their own functions. The source code of HALO_GPS software is opened for the researcher to study and communication. Additionally, for testing the installation of HALO_GPS software, some examples and standard control file templates are prepared for the user.

Although HALO_GPS Version 1.0 is well qualified to process the standard aircraft GPS data, and has strong stable, reliable, as well as high precision, it is not a strong function software until now. However, some functions (e.g. filter algorithm, network solution, precise single point positioning and GPS/INS integrated positioning) have been finished. If possible, these functions will be implemented in the HALO_GPS Version 2.0 before the end of 2010.

9. Acknowledgements

Gratefully acknowledged are the supports from Prof. Kahle, Dr. C. Föerste, Dr. F. Barthelmes, and Dr. S. Petrovic. Without their encouragements this software would never been born.

I would like to thank my advisor, Dr. Guochang Xu, for the guidance and encouragement given during my three years at GFZ. I am also grateful to him for the freedom that he gave me to explore and develop my own ideas.

My special thanks go to my other co-author, Dr. Tianhe Xu, who is an excellent young scientist. This software was significantly improved during the cooperation that we started last year. He gave a key contribution for the development of the theory and algorithm. I am also grateful to him for many discussions, which made it possible the publications of some papers in peer-reviewed journals. I wish to have in the future many other occasions to cooperate with him.

In this study are used aircraft GPS data of the airborne gravity campaign NorthGrace2007 and AlpinAero2008 carried out by BKG in cooperation with GFZ and BGR; the participating scientists and institutions are thanked for their cooperation.

Thanks Mr. Markus Ramatschi and Dr. Junping Chen of section 1.1 at GFZ for providing experimental equipments in antenna movement experiment. Thanks Hong Kong Polytechnic University for providing the data of sea buoys. And thanks Massachusetts Institute of Technology for providing GAMIT software.

Thanks my colleagues, Indridi Einarsson, Roelof Rietbroek, and Dr. Magdala Tesauro, for their help revise this manual to make it more readable.

This work was sponsored by GFZ PhD. Student Scholarship, China Scholarship Council and the Helmholtz Association of German Research Centers Council.

10. References

Boehm J., Niell A., Tregoning P., Schuh H., Global Mapping Function (GMF): A new empirical mapping function based on numerical weather model data, Geophysical Research Letter, 33, L07304, 2006.

Chen Gang, GPS Kinematic Positioning for the Airborne Laser Altimetry at Long Valley California [D], PhD thesis, 1998, Massachusetts Institute of Technology, U.S.A.

Christoph Foeste, Mirko Scheinert, A Platform for Earth Observations and Geophysics [R], DFG Priority Program 1294 “HALO”, Evaluation Colloquium, Oberpaffenhofen, Germany, 11-12, March, 2010

Collins, J. P., Langley R.B., Estimating the residual tropospheric delay for airborne differential GPS positioning, Proceedings of ION GPS-97, 1197-1206, Kansas City, Mo., 16-19 September, 1997.

Collins J. P., Assessment and development of a tropospheric delay model for aircraft rovers of the global positioning System. M.Sc.E. Thesis, Department of Geodesy and Geomatics Engineering Technical Report No.203, University of New Brunswick, Fredericton, New Brunswick, Canada, 1999.

Gendt G., Reigber C., Dick G., Near real-time water vapor estimation in a German GPS network: First results from the ground program of the HGF GASP project, Physics and Chemistry of the Earth (A), 26, 6-8, 413-416, 2001.

Gauthier L., P. Michel, J. Ventura-Traveset and J. Benedicto, EGNOS: The first step in Europe’s contribution to the global navigation satellite system, ESA Bulletin, 105, 35-42, 2001.

Hopfield H. S., Tropospheric effect of electromagnetically measured range: Prediction form Surface Weather Data, Radio Science, 6, 357-367, 1971.

Heise S., Wickert J., Beyerle G., Schmidt T., and Reigber Ch., Global monitoring of tropospheric water vapor with GPS radio occultation aboard CHAMP, Advance in Space Research, 12(37), 2222-2227, 2006.

Hu Guorong, Ovstedal O., Featherstone W.E. and et al., Using the Virtual Reference Stations Concept for Long-range Airborne GPS Kinematic Positioning [J], Survey Review, 2008, 40(307): 83-91

King R. W., Bock Y., Documentation for the GAMIT GPS analysis software version 10.03, Massachusetts Institute of Technology, 2000.

Mendes V.B., Collins P., Langley R.B., The effect of tropospheric propagation delay errors in airborne GPS precision positioning, Proceedings of ION GPS-95, the 8th International Technical Meeting of the Satellite Division of The Institute of Navigation, Palm Springs, Calif., 12-15 September, 1995.

Mendes V.B., Langley R.B., Tropospheric zenith delay prediction accuracy for airborne GPS high-precision positioning, Proceedings of ION 54th Annual Meeting, Denver, Colorado, June 1-3, pp.337-348, 1998.

Penna N., Dodson A. and Chen W., Assessment of EGNOS Tropospheric Correction Model, Journal of Navigation, 54(1), 37-55, 2001.

Saastamoinen J., Contributions to the theory of atmospheric refraction, Part II Refraction Corrections in Satellite Geodesy, Bulletin Geodesique, 107, 13-34, 1973.

Sanssen V., Ge L., Rizos C., Tropospheric delay corrections to differential INSAR results from GPS observations, 6th International Symposium on SatNav, 22-25 July, Melbourne, Australia, 2003.

Syndergaard S., Retrieval analysis and methodologies in atmospheric limb sounding using the GNSS radio occultation technique. Dissertation, Niels Bohr Institute for Astronomy, Physics and Geophysics, Faculty of Science, University of Copenhagen, 1999.

Schaefer U., Liebsch G., Schirmer U., Meuschke A., Pflug H., Wang Q., Petrovic S., Meyer U., AlpinAero2008-an airborne gravity campaign for improved geoid modelling in the Alps, EGU-2009, Vienna, Austria, 19-24 April, 2009.

Troller M., Geiger A., Brockmann E., et al., Tomographic determination of the spatial distribution of water vapor using GPS observations, Advance in Space Research, 37(12), 2211-2217, 2006.

Wanninger L., Real-time differential GPS error modeling in regional reference station networks, Proc. 1997 IAG Symposium, 86-92, Rio de Janeiro, Brazil, 1997.

Wackernagel H., Multivariate geostatistics: an introduction with applications, Springer-Verlag, 291-292, 1998.

Wang C.H., Liou Y.A., Yeh T.K., Impact of surface meteorological measurements on GPS height determination, Geophysical Research Letter, 35, L23809, 2008.

Wang Qianxin, Xu Guochang, S. Petrovic, U. Schaefer, U. Meyer, Xu Tianhe, A regional tropospheric model for

airborne GPS-applications, Advances Space Research, 2010, under review.

Wang Qianxin, Xu Guochang, Chen Zhengyan, Interpolation method of tropospheric delay of high altitude rover based on regional GPS network, Geomatics and Information Science of Wuhan University, Vol.35(11), 2010.

Wang Qianxin, Xu Tianhe, Xu Guochang, Application of robust estimation to GPS airborne kinematic relative positioning, Geomatics and Information Science of Wuhan University, 2010, under review.

Wang Qianxin, Xu Tianhe, Xu Guochang, GPS kinematic positioning for long range flight based on single baseline model, Acta Geodaetica et Cartographica Sinica, 2010, submitted.

Wang Qianxin, Xu Guochang, Real-time GPS Satellite Clock Error Prediction Based On No-stationary Time Series Model, Europe Geosciences Union (EGU), Vol.11, EGU2009-5993-1, 19th-24th, April, Vienna, Austria.

Wang Qianxin, Li Li, Gong Youxing, Study of GPS satellite clock's behaviors and prediction, Science of Surveying and Mapping, No.2, 2010.

Xu Guochang, P. Schwintzer, and Ch. Reigher, KSGSoft (Kinematic Static GPS Software)-Software User Manual, Scientific Technical Report 19/1998. GeoForschungsZentrum, Germany, 1998

Xu G., A concept of precise kinematic positioning and flight-state monitoring from the AGMASCO practice, Earth Planet Space, 52, 831-835, 2000.

Xu Guochang, GPS Data Processing With Equivalent Observation Equations [J], GPS Solutions, 2002(6): 28-33

Xu Guochang, GPS-theory, algorithms and application, 2nd Ed, Springer, 232, 2007.

Xu Tianhe, Yang Yuanxi, The hypothesis testing of scale parameter in coordinate transformation model, Geomatics and Information Science of Wuhan University, 26, 70-74, 2001.

Yang Yuanxi, Robust Estimation for Dependent Observations [J], Manuscripta Geodaetica, 1994, 19(1): 10-17

Yang Yuanxi, Zeng Anmin, Fusion Modes of Various Geodetic Observations and Their Analysis [J], Geomatics and Information Science of Wuhan University, 2008, 33(8): 771-774.

Yin H., Huang D. and Xiong Y., Regional tropospheric delay modeling based on GPS reference station network, VI Hotine-Marussi Symposium on Theoretical and Computational Geodesy, 132, 185-188, 2008.

Zhang J., Lachapelle G., Precise estimation of residual tropospheric delays using a regional GPS network for real-time kinematic applications, Journal of Geodesy, 75, 255-266, 2001.

Zheng Y., Feng Y., Interpolating residual zenith tropospheric delays for improved regional area differential GPS positioning, Proceedings of ION GPS-2005, 179-188, Long Beach, California, 2005.

11. Appendixes

11.1 Appendixes 1: Definitions of Constants

This section describes all of the constants which are used in HALO_GPS software. Part 1 introduces definitions of all constants name. Part 2 gives the special values of all constants used.

Part 1

earth_flat	--- Earth's flattening
earth_rad	--- Equatorial radius of the Earth (m)
earth_to_moon	--- Mass ratio of earth and moon
g_earth	--- Gravitational acceleration at the equator (m/s**2)
GM_moon	--- GM for moon
GM_sun	--- GM for sun
GM_earth	--- GM for Earth
G_univ	--- Gravitational constant
pi	--- Pi
rad_to_deg	--- Conversion from radians to degrees
rad_to_mas	--- Conversion from radians to milliarcseconds
sec_per_day	--- Number of seconds in 24 hours
vel_light	--- speed of light in m/s
DJ2000	--- Julian date of J2000
sec360	--- number of seconds in 360 degrees
solar_to_sidereal	--- Conversion from solar days to sidereal days (at J2000)
fL1, fL2	--- GPS frequencies in Hz at L1 and L2
dfsf, sfdf	--- Difference of frequency divided by the sum of frequencies (used form widelane and narrowlane)
lcf1, lcf2	--- Multipliers for LC from L1 and L2 frequencies
lgf1, lgf2	--- Multipliers for LG from L1 and L2 frequencies
pcf1, pcf2	--- Multipliers for PC from P1 and P2 frequencies

Part 2

```
parameter ( earth_flat     =     0.003352891869D0      )
parameter ( earth_rad      =     6378145.D0            )
parameter ( earthrot       =     7.29212E-05           )
parameter ( earth_rad      =     6378137.D0            )
parameter ( earth_flat     =     1.d0/298.257222101    )
parameter ( earth_to_moon  =     81.30065918D0         )
parameter ( g_earth        =     9.780318458D0         )
parameter ( GM_moon        =     0.49027975D+13        )
parameter ( GM_sun         =     0.132712499D+21       )
parameter ( GM_earth       =     3.986004418d+14       )
```

```
parameter   ( G_univ          =   0.66732D-10                    )
parameter   ( pi              =   3.1415926535897932D0           )
parameter   ( sec_per_day     =   86400.D0                       )
parameter   ( sec360          =   1296000.d0                     )
parameter   ( vel_light       =   299792458.D0                   )
parameter   ( DJ2000          =   2451545.d0                     )
parameter   ( solar_to_sidereal =  1.002737909d0                 )
parameter   ( fL1             =   154*10.23d6                    )
parameter   ( fL2             =   120*10.23d6                    )
parameter   ( wave1           =   vel_light/fL1                  )
parameter   ( wave2           =   vel_light/fL2                  )
parameter   ( wave_LC         =   vel_light/fL1                  )
parameter   ( wave_WL         =   vel_light/(fL1-fL2)            )
parameter   ( rad_to_deg      =   180.d0   /pi                   )
parameter   ( rad_to_mas      =   648000.d3/pi                   )
parameter   ( dfsf            =   (fL1-fL2)/(fL1+fL2)            )
parameter   ( sfdf            =   (fL1+fL2)/(fL1-fL2)            )
parameter   ( lcf1            =   1.d0/(1.d0 - (fL2/fL1)**2)     )
parameter   ( lcf2            =   -(fL2/fL1)/(1.d0 - (fL2/fL1)**2) )
parameter   ( lgf1            =   -fL2/fL1                       )
parameter   ( lgf2            =   1.d0                           )
parameter   ( pcf1            =   fL1**2/(fL1**2-fL2**2)         )
parameter   ( pcf2            =   -fL2**2/(fL1**2-fL2**2)        )
```

11.2 Appendixes 2: List of Figures

ISSN 1610-0956